

Anisotropic scattering and quantum magnetoresistivities of a periodically modulated 2D electron gas

Andrei Manolescu

Institutul Național de Fizica Materialelor, C.P. MG-7 București-Măgurele, Romania

Rolf R. Gerhardt

Max-Planck-Institut für Festkörperforschung, Heisenbergstraße 1, D-70569 Stuttgart, Germany

Michael Suhrke and Ulrich Rössler

Institute for Theoretical Physics, University of Regensburg, D-93040 Regensburg, Germany

Abstract

We calculate the longitudinal conductivities of a two-dimensional noninteracting electron gas in a uniform magnetic field and a lateral electric or magnetic periodic modulation in one spatial direction, in the quantum regime. We consider the effects of the electron-impurity scattering anisotropy through the vertex corrections on the Kubo formula, which are calculated with the Bethe-Salpeter equation, in the self-consistent Born approximation. We find that due to the scattering anisotropy the band conductivity increases, and the scattering conductivities decrease and become anisotropic. Our results are in qualitative agreement with recent experiments.

73.61.-r, 73.50.Bk, 71.70.Di

I. INTRODUCTION

Magnetotransport properties of two-dimensional electron gases (2DEGs) at semiconductor interfaces, subjected to one-dimensional lateral superlattices defined by periodic electrostatic or magnetostatic fields, have attracted increasing interest during the last decade. Properties like the commensurability (Weiss) oscillations of the magnetoresistance¹ or the low-field positive magnetoresistance² are well understood and have been qualitatively explained both by quantum-mechanical^{3–6} and by classical transport calculations.^{7,8} These interesting effects occur at low temperatures (about 4 K or below), where the transport properties are governed by random-impurity scattering. It is well known that in the high-mobility 2DEGs at semiconductor interfaces the basic scattering mechanism is due to long-range Coulomb impurities, which lead predominantly to small-angle scattering of the electrons. In all the mentioned papers this aspect has, however, been neglected and the electron-impurity scattering has been treated within simplified, phenomenological models, related to a simple relaxation-time approximation. Such models are suitable only for short-range (delta-potential) impurities, which lead to isotropic scattering, in contrast to the anisotropic scattering implied by realistic impurities.

Only the most recent calculations, based on classical mechanics and Boltzmann equation, have proven that an adequate treatment of scattering anisotropy is important for an understanding of the experimental data. For instance, the number and the amplitude of the resolved Weiss oscillations of the resistivity component ρ_{\perp} , measured when the current flows *perpendicular* to the superlattice (i.e., perpendicular to the direction of translational invariance), can be fitted only if a strongly anisotropic scattering is assumed.^{9,10} Although in the regime of Weiss oscillations the magnetic fields are apparently weak enough to allow for classical calculations, quantum effects determined by the Landau quantization also play a role in this regime. The (weaker) oscillations of the resistivity component ρ_{\parallel} , which are observed when the current flows *parallel* to the superlattice and have a phase opposite to those of ρ_{\perp} , have been explained by the quantum oscillations in the density of states (DOS).^{1,4} For stronger magnetic fields, the presence of well defined Landau bands has been clearly identified also in the perpendicular resistance.^{11,12} More recently, periodic magnetic fields with extremely strong gradients, of amplitudes up to 0.4 T and periods of 500 nm, have been obtained, and huge magnetoresistance oscillations have been detected,¹³ presumably of a quantum origin. Experiments on another class of unidirectional (electrostatic) superlattices, of short-periods, have shown an anisotropy of the magnetoresistivity tensor which could be explained, within a semi-classical theory, by different transport times in the directions perpendicular and parallel to the superlattice, and ascribed to the anisotropic character of the scattering events.¹⁴

Previous quantum-mechanical calculations for modulated systems have treated the electron-impurity self-energy as a simple c-number.^{4,12,15} Strictly speaking, this is correct only for delta impurities in the unmodulated system, whereas for modulated systems even in the simple self-consistent Born approximation and for delta impurities a complicated self-energy operator results, which does neither commute with the Hamiltonian of the impurity-free modulated system, nor with the Green function operator of the impurity averaged system. The assumption of a c-number self-energy may be sufficient to explain certain aspects of the influence of a periodic modulation on the magnetoresistivities qualitatively,

especially for a weak modulation. For a strong modulation however, it can not be justified and will lead to incorrect results. Moreover, to include the effect of strongly anisotropic impurity scattering, which turned out to be important in the classical calculations, we have to consider long-range impurity potentials, which lead to important current vertex corrections and are not compatible with a c-number approximation for the self-energy.

In this paper we take the mentioned experimental information as a motivation to perform a quantum-mechanical transport calculation with a more elaborated treatment of the electron-impurity scattering, including the scattering anisotropy. We shall consider only modulations of the 2DEG varying along one lateral direction, partly because this is a situation of considerable experimental relevance, but also since we expect in this situation especially strong anisotropy effects resulting from the interplay of anisotropic periodic modulation and anisotropic impurity scattering. We use the Kubo formalism, and we calculate the electron-impurity self-energy in the self-consistent Born approximation (SCBA), on the same footing with the vertex function, with a numerical scheme based on Fourier expansions. For technical reasons we describe the finite-range impurities by Gaussian potentials. After recalling the simplest and most important classical results (Sec. II and Appendix B), we describe our calculations (Sec. III and Appendix A), and then we discuss examples with electric and magnetic modulations (Sec. IV). Finally we close with some general conclusions (Sec. IV).

II. SIMPLE CLASSICAL RESULTS

We sketch briefly the simplest results concerning the effect of the scattering anisotropy in transport. For the homogeneous, unmodulated system, the best known expressions for the conductivities of the 2DEG in a magnetic field are the classical Drude formulas,

$$\sigma_{xx} = \sigma_{yy} = \frac{\sigma_0}{1 + (\omega_c\tau)^2}, \quad -\sigma_{xy} = \sigma_{yx} = \omega_c\tau\sigma_{xx}, \quad (2.1)$$

$\sigma_0 = ne^2\tau/m$ being the zero-field conductivity, and $\omega_c = eB_0/m$ the cyclotron frequency in the externally applied perpendicular magnetic field B_0 . n is the electron density, τ is the relaxation time, and m is the conduction-band effective mass. For $\omega_c\tau \gg 1$ the diagonal conductivities are proportional to the scattering rate, $\sigma_{xx}, \sigma_{yy} \sim 1/\tau$, resulting from transitions of electrons between closed cyclotron orbits, mediated by electron-impurity scattering. Those contributions to the conductivity will be called scattering contributions in the following. In the presence of a (weak) modulation in x direction, the guiding centers of the cyclotron orbits perform a drift motion in y direction. This drift leads to an additional contribution to σ_{yy} , which in the simplest approximation⁷ can be written as average of the square of the drift velocities taken over all drifting orbits at the Fermi energy E_F ,

$$\Delta\sigma_{yy} = \frac{e^2n\tau}{E_F} \langle \bar{v}_y^2 \rangle. \quad (2.2)$$

Being due to open orbits with a finite velocity, the modulation induced contribution $\Delta\sigma_{yy}$ is, similar to σ_0 , proportional to the scattering time τ itself and not to its inverse as σ_{xx} . These different τ dependences lead us to expect peculiar anisotropies of the conductivity tensor in the presence of anisotropic impurity scattering.

For isotropic electron-impurity scattering, the relaxation time in Eq. (2.1) is the average flight time of an electron between two scattering events, $\tau = \tau_{sc}$. For anisotropic scattering this has to be replaced by the transport or momentum relaxation time, $\tau = \tau_{tr}$, which is given by

$$\frac{1}{\tau_{tr}} = \frac{1}{\tau_{sc}} \int_{-\pi}^{\pi} \frac{d\theta}{2\pi} w(\theta; k_F) (1 - \cos\theta), \quad (2.3)$$

where w is the scattering amplitude for elastic scattering at the Fermi edge from an initial state \mathbf{k}_i to a final state \mathbf{k}_f , which depends only on $|\mathbf{k}_f| = |\mathbf{k}_i| = k_F$ and the angle θ between \mathbf{k}_f and \mathbf{k}_i . For isotropic scattering, $w(\theta; k_F) \equiv 1$, and $\tau_{tr} = \tau_{sc}$. In general, however, $\tau_{tr}/\tau_{sc} > 1$, and this ratio increases with increasing predominance of small-angle scattering. This means that with increasing importance of forward scattering, and for $\omega_c\tau \gg 1$, the conductivity component σ_{xx} and the scattering contribution to σ_{yy} should become smaller,¹⁶ whereas $\Delta\sigma_{yy}$ is expected to become larger, similar to σ_0 .

Corresponding anisotropies are expected for the resistivity tensor

$$\rho_{xx(yy,xy)} = \frac{\sigma_{yy(xx,yx)}}{\sigma_{xx}\sigma_{yy} + \sigma_{xy}^2}. \quad (2.4)$$

For the homogeneous system, the classical Drude resistivity tensor has diagonal components which are independent of the magnetic field, $\rho_{xx} = \rho_{yy} = 1/\sigma_0$, and thus always *decrease* with increasing importance of forward scattering. A simple argument for this result is that the dominant contribution to the electrical resistance comes from the electron backscattering while the forward scattering gives no contribution. Obviously, for finite-range impurities the scattering anisotropy favors the forward-scattering events. For a system with periodic modulation in x direction, the classical calculations^{7,9} yield a modulation-induced contribution $\Delta\rho_{xx}$ which, in contrast to $1/\sigma_0$, *increases* with increasing forward scattering.

It has also been emphasized in Refs.^{7,9} that, even for isotropic scattering, the backscattering term in Boltzmann's equation does not vanish as in homogeneous systems, but rather is important to guarantee particle conservation, i.e., the equation of continuity. This backscattering term, which is the classical analog of the vertex corrections in the quantum treatment, is necessary to obtain the correct (quasi-local) B_0 dependence of the modulation-induced resistance correction for large magnetic fields, which is $\Delta\rho_{xx}/\rho_0 \sim (B_0)^2$ for electric and $\Delta\rho_{xx}/\rho_0 \sim (B_0)^0$ for pure magnetic modulation.⁹ The simplistic approximation of Eq. (2.2) is not in accord with the equation of continuity and yields asymptotic results which are by a factor proportional to $(B_0)^{-2}$ too small.⁹ These deficiencies become important if B_0 becomes so large that the cyclotron diameter $2R_c$ of electrons at the Fermi level becomes smaller than the modulation period a .^{7,9}

III. KUBO FORMULA AND SELF-CONSISTENT EQUATIONS

The Hamiltonian of an electron situated in the (x, y) plane, in the presence of modulating magnetic and electric fields is

$$H = \frac{1}{2m} [\mathbf{p} + e\mathbf{A}(x)]^2 + V(x). \quad (3.1)$$

The electric and magnetic modulations are defined by a periodic potential, $V(x) = V(x+a)$, and by a magnetic field with periodic z component $B(x) = B(x+a)$, respectively. We always assume a non-vanishing average value $B_0 \neq 0$ of $B(x)$, and we shall denote by $\ell = (\hbar/eB_0)^{1/2}$ the corresponding magnetic length. For the vector potential we use the Landau gauge, $\mathbf{A}(x) = (0, \int_0^x B(x')dx')$. In absence of the modulation the eigenstates are the well-known Landau states $|nX_0\rangle$ [see Eq. (A1)] with center coordinates $X_0 = -\ell^2 p_y/\hbar$, where p_y is the conserved canonical momentum. The modulation lifts the degeneracy with respect to X_0 , which however remains a good quantum number due to the translational invariance in the y direction. The energy spectrum becomes structured in periodic bands, $E_{n,X_0} = E_{n,X_0+a}$, with the corresponding modified eigenstates $|nX_0\rangle$. Such modulation-induced bands have recently been calculated for arbitrarily strong pure and mixed electric and magnetic modulations, and the energy spectra and eigenstates have been related to the different types of corresponding classical orbits.¹⁷ In the following, we will have to distinguish between two relevant basis sets of the Hilbert space, the *Landau basis* $\{|nX_0\rangle\}$ of eigenstates of the homogeneous 2DEG, and the *modulated basis* $\{|nX_0\rangle\}$ of eigenstates of the modulated 2DEG.

We apply the standard procedure of averaging the retarded (advanced) Green's functions over all the configurations of randomly distributed impurities, $G^\pm \equiv \langle \hat{G}^\pm \rangle_{imp}$, where $(\hat{G}^\pm)^{-1}(E) = E - H - V_{imp} \pm i0^+$ and V_{imp} is the potential describing a given impurity configuration. This leads, in the simplest consistent approximation, to the coupled equations

$$(G^\pm)^{-1}(E) = E - H - \Sigma^\pm(E), \quad (3.2)$$

$$\Sigma^\pm(E) = n_i \int d\mathbf{R} u(\mathbf{r} - \mathbf{R}) G^\pm(E) u(\mathbf{r} - \mathbf{R}). \quad (3.3)$$

Equation (3.2) defines the self-energy operator $\Sigma^\pm(E) = \Delta(E) \mp i\Gamma(E)/2$. The spectral operator $A(E) = [G^-(E) - G^+(E)]/(2\pi i)$ and $\Gamma(E)$ are positive (semi-)definite Hermitean operators. The DOS is $D(E) = D_0 \hbar \omega_c / (\pi a) \sum_n \int_0^a dX_0 (nX_0 | G^-(E) | nX_0)$, where $D_0 = m/(\pi \hbar^2)$. Equation (3.3) is the SCBA, the self-consistent approximation of the lowest order in the impurity concentration n_i , u being the electron-impurity potential.

The diagonal conductivities are calculated from the Kubo formula,^{16,18,19}

$$\begin{aligned} \sigma_{\alpha\alpha} &= \int dE \left[-\frac{d\mathcal{F}(E)}{dE} \right] \sigma_{\alpha\alpha}(E), \\ \sigma_{\alpha\alpha}(E) &= \frac{e^2 \hbar}{2\pi} \frac{1}{L_x L_y} \text{Tr} \left\{ v_\alpha \left[2F_\alpha^{+-}(E) - F_\alpha^{++}(E) - F_\alpha^{--}(E) \right] \right\}, \end{aligned} \quad (3.4)$$

where $\alpha = x, y$, L_x and L_y are the linear dimensions of the 2DEG, \mathcal{F} is the Fermi function, v_α is the velocity operator, and spin-degeneracy is assumed. The vertex functions $F_\alpha^{\sigma\sigma'} \equiv \langle \hat{G}^\sigma v_\alpha \hat{G}^{\sigma'} \rangle$ with $\sigma = \pm$ are given by the equations

$$F_\alpha^{\sigma\sigma'}(E) = G^\sigma(E) v_\alpha G^{\sigma'}(E) + G^\sigma(E) I[F_\alpha^{\sigma\sigma'}(E)] G^{\sigma'}(E), \quad (3.5)$$

$$I[F_\alpha^{\sigma\sigma'}(E)] = n_i \int d\mathbf{R} u(\mathbf{r} - \mathbf{R}) F_\alpha^{\sigma\sigma'}(E) u(\mathbf{r} - \mathbf{R}), \quad (3.6)$$

which are similar to Eqs. (3.2) and (3.3). Equation (3.5) is the Bethe-Salpeter equation for the vertex function, and Eq. (3.6) defines the vertex corrections $I[F_\alpha^{\sigma\sigma'}(E)]$ in the SCBA. A

diagrammatic formulation of the SCBA is shown in Fig. 1. It is sufficient for calculations of the conductivity if interference effects such as weak or strong localization are not important.

As a simple and easily tractable model for the impurity potential, we use a Gaussian model,

$$u(\mathbf{r}) = \frac{u_0}{\pi r_0^2} e^{-(r/r_0)^2}, \quad \tilde{u}(\mathbf{q}) = u_0 e^{-(qr_0)^2/4}, \quad (3.7)$$

where \tilde{u} is the Fourier transform. Within the SCBA, the scattering effect of randomly distributed impurities of density n_i is described by only two parameters, an energy $\Gamma_0^0 = n_i u_0^2 m / \hbar^2$ which determines $\tau_{sc} = 2\hbar / \Gamma_0^0$ in Eq. (2.3), and the impurity range r_0 . In the presence of a strong perpendicular magnetic field, these parameters enter the equations for the Green's functions and the conductivities via the energy $\Gamma_0 = \sqrt{\Gamma_0^0 \hbar \omega_c} = \sqrt{n_i} u_0 / \ell \equiv \gamma \sqrt{B_0}$, which determines the scattering-induced broadening of the spectrum, and the length ratio r_0 / ℓ , which determines the anisotropy of the impurity scattering.¹⁶ This model allows a direct comparison between the results for point-like ($r_0 = 0$) and finite-range ($r_0 \neq 0$) impurities. Major simplifications of the transport calculation occur only for the unmodulated system and $r_0 = 0$. A direct inspection of Eqs. (3.2)-(3.6) shows that in this case the self-energy operator becomes a simple (energy-dependent) c-number, and the current vertex corrections, Eq. (3.6), vanish.^{16,18}

A. The usual 'c-number approximation'

Although this is no longer true in the presence of a modulation, even if δ -impurities are assumed, the ansatz that the self-energy is still a c-number (i.e., independent of all the quantum numbers), has been used quite often.^{4,12,15,20} A justification of the c-number approximation (CNA) may be that, besides its simplicity, it is exact (for δ -impurities) in the limit of zero modulation and, therefore, may be reasonable also for sufficiently weak modulations. This ansatz is sufficient to ensure the vanishing of the vertex corrections, but, on the other hand, it captures essential effects of the collisions and of the density of states.⁴ Moreover, it is regarded as satisfactory if one is interested mainly in the influence of the system geometry and not of impurity scattering on the transport properties. In the CNA the Green function operator is diagonal in the modulated basis, $(nX_0|G^\sigma(E)|n'X_0) = \delta_{n,n'} G_{nn}^\sigma(X_0, E)$, such that the longitudinal conductivities may be written as

$$\sigma_{\alpha\alpha}(E) = \frac{\hbar e^2}{\pi^2 \ell^2} \int_0^a \frac{dX_0}{a} \sum_{nn'} |(nX_0|v_\alpha|n'X_0)|^2 \text{Im}G_{nn}^-(X_0, E) \text{Im}G_{n'n'}^-(X_0, E). \quad (3.8)$$

In this expression the essential difference between σ_{xx} and σ_{yy} , generated only by the anisotropy of the modulation, is determined by the diagonal ($n = n'$) contribution which exists only for $\alpha = y$, since $(nX_0|v_x|nX_0) = 0$. This intra-Landau-band contribution, also known as *band conductivity*,²¹ is related to the net motion of electrons in the direction perpendicular to the electric field and/or the gradient of the magnetic field defining the modulation, with the group velocity

$$(nX_0|v_y|nX_0) = -\frac{1}{m\omega_c} \frac{dE_{n,X_0}}{dX_0}. \quad (3.9)$$

If the scattering broadening Γ_0 is much smaller than the modulation-induced bandwidth of the Landau levels, and if this in turn is so small that adjacent Landau bands do not overlap, simple estimates of the dependence of the different conductivity contributions on Γ_0 and the DOS at the Fermi level, $D(E_F)$, are available. As shown in Appendix B, the band conductivity diverges for $\Gamma_0 \rightarrow 0$ like $[\Gamma_0 D(E_F)]^{-2}$ (provided E_F is inside a Landau band and not too close to a band edge). This explains – in the quantum treatment – the Weiss oscillations, with minima when E_F intersects a flat band.⁴ The inter-Landau-band contribution to Eq. (3.8) ($n \neq n'$), also known as *scattering conductivity*, in general behaves like $[\Gamma_0 D(E_F)]^2$, and entirely determines σ_{xx} . Within the CNA, for a sufficiently clean system (small Γ_0), the scattering conductivity σ_{yy}^{scat} is much smaller than the band conductivity at weak magnetic fields, i.e., in the regime of the Weiss oscillations, and both conductivity contributions may become comparable for strong fields, in the regime of the Shubnikov - de Haas (SdH) oscillations. Also, the scattering conductivities are almost the same in the modulated and unmodulated directions.²²

For large B_0 , the estimates given in Appendix B yield $\sigma_{yy}^{band} \sim (B_0)^{-2}$ for pure electric and $\sigma_{yy}^{band} \sim (B_0)^{-4}$ for pure magnetic modulation, leading to $\Delta\rho_{xx}/\rho_0 \sim (B_0)^2$ and $\Delta\rho_{xx}/\rho_0 \sim (B_0)^0$, respectively. All these results for the CNA are in agreement with the corresponding classical results summarized in Sec. II. This confirms our expectation, that consideration of vertex corrections is important, not only from a quantitative point of view, in order to include the effect of anisotropic scattering, but also from a qualitative point of view, to avoid violation of the equation of continuity. The neglect of vertex correction, e.g., in the CNA, leads to uncontrolled and (at least for large B_0) unacceptable results, even for isotropic scattering.⁹ The deficiencies of the CNA also became clear from a quantitative comparison between experimental results and quantum-mechanical calculations which were non-perturbative with respect to the periodic modulation potential.¹⁵ In that work it turned out to be impossible to fit the magnitude of the experimental resistance and the dominance of scattering conductivity over band conductivity (indicated by resistance *minima* at the flat band conditions) at the same time.

B. Beyond the CNA

The aim of the present paper is to go beyond the CNA. Indeed, there exists no justification of the CNA within the formalism of the SCBA. Even if we *assume* that the Green operator (3.2) is diagonal, say in the modulated basis, and insert that into Eq. (3.3), the evaluation of the kernel (see Appendix A) yields a non-diagonal self-energy, and thus in the next iteration step a non-diagonal Green operator. One finds, that there exists no basis in which the Hamiltonian of the modulated system (without disorder), the impurity-averaged Green function, and the self-energy operator are simultaneously diagonal, since these three operators do all not commute with each other. For obtaining numerical solutions of the self-consistent equations (3.2)-(3.3) and (3.5)-(3.6) we find it convenient to express the matrix elements of all the operators in the Landau basis, since the kernels describing the impurity-averaging in the SCBA are independent of the modulation in this case.

Then, for a given modulation model and for fixed values of energy E and average magnetic field B_0 , the matrix elements of the Green operator $\langle m, X_0 | G^\sigma(E) | n, X'_0 \rangle = \delta_{X'_0, X_0} G_{m,n}^\sigma(X_0, E)$ depend on two discrete (Landau) quantum numbers and a quasi-

continuous one (center coordinate). Equation (3.3) provides a linear relation between these and the self-energy matrix elements, which have the same structure, mediated by the SCBA kernel, which depends on four discrete indices and a single continuous one, since the X_0 relation is of a convolution type (see Appendix A). Thus, it is convenient to expand the X_0 dependence into a Fourier series. Moreover, we restrict our consideration to modulation models of defined parity, which allows to reduce the number of Fourier coefficients by a factor of two. Eqs. (3.2)-(3.3) provide a non-linear integral equation for $G_{m,n}^\sigma(X_0, E)$ or, equivalently, $\Sigma_{m,n}^\sigma(X_0, E)$. At finite temperature, the solutions are needed in a finite interval around the chemical potential, which has to be calculated for given average electron density. Having calculated these solutions, we can solve the linear integral equations (3.5)-(3.6) for the vertex functions, which have a similar matrix structure as the Green operator and are needed to calculate the conductivity components. It is evident that the requirements on storage capacity and computational time increase rapidly with the number of Landau levels and of Fourier coefficients, which have to be taken into account. Due to the limited computer facilities, we will therefore have to use somewhat unrealistic model assumptions, which allow to restrict, e.g., the number of necessary Fourier coefficients. We will also restrict the investigation of scattering-anisotropy effects to the consideration of only two values of the impurity range r_0 . The results of the CNA can be found by taking $r_0 = 0$ and, simultaneously, reducing all the Fourier series to the first term with $p = 0$ (which is the average value, see Appendix A). Note, that the latter prescription is an additional approximation which has no justification, but allows the comparison of the correct results with those of the CNA.

We shall consider the effects of the anisotropic collisions on the scattering and band contributions to the diagonal components of the *conductivity tensor*. In order to illustrate the results for the *resistivity tensor*, Eq. (2.4), we shall simplify the Hall conductivity by completely neglecting the impurity effects on it. Of course, quantum Hall plateaus are thus ignored, although they are seen in the experiments on modulated systems for larger magnetic fields. However, we assume that the structure of the longitudinal resistivities is mostly determined by the periodic Landau bands for sufficiently low magnetic fields, and not by localization effects which are beyond the SCBA. Especially the anisotropy effects corresponding to the band conductivity are expected to result from the diagonal components of the conductivity tensor (a corresponding diagonal contribution in the modulated basis does not exist for the Hall conductivity). With these assumptions, the Hall conductivity is given by

$$\sigma_{xy} = \frac{2i\hbar e^2}{\pi\ell^2} \int_0^a \frac{dX_0}{a} \sum_{n \neq n'} \mathcal{F}(E_{nX_0}) \frac{(nX_0|v_x|n'X_0)(n'X_0|v_y|nX_0)}{(E_{nX_0} - E_{n'X_0})^2}. \quad (3.10)$$

IV. RESULTS

For computational reasons we have chosen our modulation parameters such that we can obtain convergent results by truncating the Landau basis to the first 10-30 wave functions, and the Fourier series with respect to X_0 to the first 10-20 terms. We avoid the necessity of including higher Fourier coefficients by keeping a relatively weak modulation amplitude, and also by choosing r_0 shorter, but comparable to ℓ . For a disorder broadening much smaller

than the typical bandwidth, the periodic matrix elements $G_{nn'}^\sigma(X_0, E)$ and $F_{nn'}^{\sigma\sigma'}(X_0, E)$ as functions of X_0 exhibit large pole-like structures (which become poles for $\Gamma_0 \rightarrow 0$), if E falls into the spectrum E_{m, X_0} of the Landau bands $m = n$ or $m = n'$. Apparently this structure requires the inclusion of many Fourier coefficients. But, due to the Gaussian factors of the Landau wave functions, the matrix elements of the collision operator Γ^2 decay like Gaussians with increasing $|X_0 - X'_0|$, Eq. (A3), and thus the higher-order Fourier amplitudes have a vanishing (also Gaussian) contribution to $\Sigma_{nn'}^\sigma(X_0, E)$ and $I[F_{nn'}^{\sigma\sigma'}(X_0, E)]$, respectively. This can be directly seen on the analytical results available for $r_0 = 0$, Eqs. (A10) and (A7). For $r_0 \neq 0$ the Fourier coefficients are calculated by integrating the periodic functions, and in order to keep a reasonable number of points in the integrals we restricted ourselves - nevertheless - to a relatively large disorder broadening, i.e., Γ_0 smaller, but comparable to the width of the Landau bands. Therefore, we do not attempt to give necessarily realistic results, but rather to identify and to understand the effects of the anisotropic scattering qualitatively.

A. Electric modulation

We start with an example of a pure electric modulation ($B(x) \equiv B_0$), determined by the electrostatic potential $V(x) = U \cos(2\pi x/a)$, with $U = 0.8$ meV and $a = 400$ nm. The material parameters are for GaAs: $m = 0.067m_0$, the electron density ($n_{\text{el}} = 1.93 \cdot 10^{11} \text{ cm}^{-2}$, $E_F(B_0=0) = 6.91$ meV) chosen such that $\nu B_0 = 8$ T, ν being the filling factor, and we assume spin degeneracy. We fix the temperature to 1 K, and the disorder parameter $\gamma = 0.5$ meV T $^{-1/2}$ corresponding to a mobility $\mu = 2.2 \cdot 10^5 \text{ cm}^2/Vs$ at $B_0 = 0$ in CNA and to an increasingly larger mobility with growing anisotropy of scattering as the ratio τ_{tr}/τ_{sc} increases.

In Fig. 2 we show $D(E_F)$ and a typical energy spectrum, with $B_0 = 0.81$ T so that the Fermi level is in the Landau bandwidth $n = 4$. We compare the CNA with the results of the calculations with a matrix self-energy for $r_0 = 0$ (delta impurities) and for a finite r_0 . Broadened van Hove singularities (VHS's) are resolved in all cases. The small maximum at $B_0 = 0.9$ T is an artifact due to the elliptic shape of the DOS, typical for the SCBA: unlike in the CNA, in the other calculations the self-energy depends on the center coordinate, and since the disorder broadening is comparable to the bandwidth, the two high-DOS peaks due to the band edges may partially overlap, yielding extra maxima in between. Such details are, however, not important for the conductivities.

Results for the conductivities are shown in Fig. 3, again in the CNA, and also with a matrix self-energy (including the vertex corrections), for two choices of r_0 . Note, that the Landau bands do not overlap in the present case. Thus, in the CNA the scattering and band conductivities are given by the estimates Eqs. (B7) and (B11) in Appendix B. Numerically, we obtain $\sigma_{xx} \approx \sigma_{yy}$ in the CNA, which tells that, *in this approximation* and for the chosen values of modulation amplitude and (relatively large) disorder broadening, the band conductivity is very small. The first flat-band condition (see Appendix B) at E_F is obtained for $B_0 \approx 0.5$ T, where the scattering conductivities have maxima. When the vertex corrections are included, even for $r_0 = 0$, the situation completely changes: with increasing magnetic field the two conductivities have opposite evolutions. The pure scattering conductivity σ_{xx} is drastically reduced, and the band conductivity leads to a

dramatic increase of σ_{yy} . While the double-peak structure of the DOS is no longer resolved in σ_{xx} , it may survive in σ_{yy} .

We can interpret these results in physical terms, taking into account that the anisotropy of the modulation results in anisotropic electron states: unbound propagation in the y direction and confined cyclotronic motion in the x direction within the cyclotron diameter $2R_c = 2\ell\sqrt{2n+1}$. For low magnetic fields such that $2R_c \gg a$ the effect of the modulation on the scattering events is averaged out and the scattering remains isotropic for $r_0 = 0$. This changes for $2R_c \ll a$, when the electrons propagate along relatively narrow channels in the y direction. The *decrease* of σ_{xx} , with respect to the CNA, can be understood just like the effect of the scattering anisotropy on the longitudinal (scattering) conductivities in the absence of the modulation, but in the presence of the magnetic field.¹⁶ At the same time, the *increase* of the band conductivity contributing to σ_{yy} can be understood in analogy to the effect of the scattering anisotropy on the conductivity of quasi-free electrons, with no modulation and no magnetic field. A Landau band has the strongest dispersion in its center and an uncertainty in energy due to disorder broadening translates into a much smaller range $\Delta k_y \sim \Delta X_0$ of available final states after scattering as compared to the band edges. This in turn leads to a stronger increase in forward scattering and, thus, to the enhanced band conductivity in the middle of a band. Obviously, this effect is stronger for finite-range impurities than for $r_0 = 0$. The decomposition of σ_{yy} into scattering and band contributions is however complicated by the vertex corrections, which in fact with increasing modulation amplitude mix them increasingly together. Therefore the behavior of the scattering contribution to σ_{yy} cannot be very clearly identified and understood with these simple interpretations.

We found numerically that, for the results shown in Figs. 3 and 4, the vertex corrections corresponding to $I[F_\alpha^{++}]$ and $I[F_\alpha^{--}]$ are negligible. For delta impurities one can show analytically that they vanish exactly for $\alpha = x$ (see Appendix A). In general, their small values can be explained with the help of the Ward identities, which relate $I[F_\alpha^{\sigma\sigma}]$ to the commutators of the self-energy with the position operators.¹⁸ The matrix elements of the vertex corrections become determined by differences between off-diagonal matrix elements of the self-energy, which are small unless the Landau-level mixing is very strong. So practically all the anisotropy effects obtained for the electric modulation are determined by $I[F_\alpha^{-+}]$.

In general, the resistivities reproduce the structure of the conductivities, according to Eq. (2.4) where the denominator is in fact given by the square of the Hall conductivity. ρ_{xx} is qualitatively similar to σ_{yy} , and ρ_{yy} to σ_{xx} respectively. Qualitatively, the results confirm the expectations, which we deduced from the analysis of the classical and the CNA results: anisotropic scattering reduces the transport scattering rate and thus reduces the scattering conductivity (and consequently σ_{xx}) and increases the band conductivity (and thus σ_{yy}). For $\Gamma_0^0 \ll \hbar\omega_c$, this should enhance ρ_{xx} , see Fig. 4 and Fig. 5(a), but lower ρ_{yy} , see Fig. 5(b). In particular, for $r_0 = 0$, the strong enhancement of ρ_{xx} over the CNA result observed at larger B_0 values in Fig. 4, also agrees with the predictions based on Boltzmann's equation: the neglect of backscattering (i.e., vertex corrections, as in the CNA), which violates the equation of continuity, results in too small values for ρ_{xx} and becomes increasingly important with increasing B_0 .

B. Magnetic modulation

In the following examples we consider a pure magnetic modulation ($V(x) \equiv 0$), defined by a periodic magnetic field of the form $B(x) = B_0 + B_1 \cos(2\pi x/a)$. We shall discuss two cases, first with a high and then with a low band conductivity, in order to separate the anisotropy effects, and also to compare with the available experimental results.

1. The regime of high band conductivity

We choose the modulation parameters comparable to those in the experiment by Ye et al. on strongly magnetically modulated 2DEG.¹³ The experiment shows huge oscillations of the magnetoresistivity ρ_{xx} for values of the average magnetic field B_0 in the intermediate regime between that of positive magnetoresistance and that of distinct SdH peaks. The positive magnetoresistance effect is also huge and covers the Weiss oscillations. In general, for both electric and magnetic modulations, the positive magnetoresistance and the Weiss oscillations have been successfully explained by the classical transport calculations, where the classical analog of the band conductivity is in fact calculated.⁷⁻¹⁰ In the intermediate regime mentioned here, the quantum effects become important. The modulated magnetic field is strong and generates Landau bands that partially overlap, yielding oscillations of the DOS at the Fermi level. We ascribe the huge oscillations observed in the experiment to the resulting oscillations of the band conductivity.

In our calculations we take $a = 400$ nm and $B_1 = 0.23$ T for the modulation, and $\gamma = 0.3$ meV T^{-1/2} for the scattering-energy parameter. In Fig. 5 we show the calculated resistivities with B_0 starting at the end of the positive-magnetoresistance regime. The vertex corrections are included, both for zero and finite impurity range. The contribution of the scattering conductivity is negligible in σ_{yy} , and thus in ρ_{xx} [see Eq. (2.4)], because the Landau bands are much wider than the disorder broadening Γ_0 . The filling factor varies between 21 and 11.4, and the number of Landau bands intersected by the Fermi level, for a fixed B_0 , varies between four and two.

In Fig. 6(a) we have selected three energy spectra with a VHS at the Fermi level, corresponding to a Landau band edge. The singularities are well resolved in $D(E_F)$, Fig. 6(b). The profile of $D(E_F)$ is very well reproduced in both resistivities calculated at zero temperature, Fig. 5. ρ_{xx} has minima and ρ_{yy} has maxima where $D(E_F)$ has maxima. This clearly tells that ρ_{xx} is determined by the band conductivity and ρ_{yy} by the scattering conductivity. For a finite temperature, like 1 K, the VHS are smeared and the resistivities oscillate according to the number of the Landau bands at the Fermi level. For instance, for 0.442 T $< B_0 < 0.473$ T *three* Landau bands are intersected by the Fermi level, while for 0.473 T $< B_0 < 0.504$ T *four* bands, Fig. 6(a), such that ρ_{xx} has a maximum in the first interval (low $D(E_F)$) and a minimum in the second one (high $D(E_F)$), while ρ_{yy} has the opposite evolution.

Just like in the case of the electric modulation, the effect of the scattering anisotropy and of the vertex corrections is to increase the band conductivity and to decrease the scattering contributions. Here, such effects are not so important for $r_0 = 0$, due to the relatively low average magnetic field. Therefore the DOS-induced oscillations of the resistivities can be qualitatively explained even in the CNA (not shown in Fig. 5; compare the estimate for

the band conductivity in the case of overlapping bands, Eq. (B12) in Appendix B), and the oscillations can be amplified by reducing the disorder parameter γ . Of course, quantitative agreement with the experiment cannot be expected in our calculations, where the disorder parameters are chosen according to computational possibilities rather than to experimental requirements. The model of Gaussian impurities involves two parameters, r_0 and $\gamma \sim \sqrt{n_i}u_0$. For a direct comparison between the theoretical and the experimental results, for different choices of r_0 one should also adjust γ , e.g. by imposing a fixed zero-magnetic-field resistance. This is given by the transport time τ_{tr} , Eq. (2.3), which can be calculated analytically for our Gaussian impurity model. To keep τ_{tr} fixed, we should compare the results for $r_0 = 10$ nm and $\gamma = 0.3$ meV T^{-1/2} with those for $r_0 = 0$ and $\gamma \approx 0.05$ meV T^{-1/2}. Of course, the realistic scatterers have a long range, with Coulomb tails determined by the spacer width, and may be not too well approximated by Gaussians.

Experimental results in this regime exist only on the resistivity component ρ_{xx} , not on ρ_{yy} , to our knowledge. We predict that, as indicated by our calculations, ρ_{yy} should be at least one order of magnitude smaller than ρ_{xx} and should oscillate in a similar manner, but with minima and maxima interchanged. Unlike the Weiss oscillations, which are determined by the geometric commensurability of the cyclotron diameter with the modulation period,¹ these novel modulation-induced oscillations occur for Fermi energies below the lowest commensurability (flat-band) condition, and are essentially a DOS effect.

2. The regime of low band conductivity

Measurements of the magnetoresistance in both x and y directions, in the quantum regime, have been recently performed on magnetically modulated 2DEGs in InAs heterostructures.^{23,24} The electron density is typically one order of magnitude higher than in GaAs systems, and thus the filling factors are much larger. The SdH peaks observed in ρ_{xx} are about 20 times higher than in ρ_{yy} . At the same time, with decreasing the uniform field B_0 , the SdH minima at even filling factors are replaced by resistivity maxima, while the minima shift to odd filling factors. It has been convincingly demonstrated, that these minima are not due to spin splitting, which in fact is not resolved in this case. A similar even-odd shift has been observed in electrically modulated systems, and explained by the behavior of the scattering conductivity when two Landau bands partially overlap. The overlapping VHS of adjacent Landau bands yield maxima instead of SdH minima, while minima occur for E_F in the middle of a band (lower DOS).¹² We therefore believe that, similarly, also in the experiment of Heisenberg et. al.,^{23,24} only the scattering conductivities are observed, and thus the big difference between ρ_{xx} and ρ_{yy} is not due to the band conductivity, but due to an anisotropy of the scattering contributions to ρ_{xx} and ρ_{yy} .

We use the parameters of InAs, $m = 0.023 m_0$, an electron density such that $\nu B_0 = 75$ T, and spin degeneracy. For the magnetic modulation we take $a = 300$ nm and $B_1 = 0.1$ T. We calculate the resistivities in the regime of the SdH oscillations for impurity parameters suitable to obtain dominant contributions from the scattering conductivities: $r_0 = 5$ nm and two values for the disorder broadening, $\gamma = 5$ meV T^{-1/2} and $\gamma = 6$ meV T^{-1/2}. The resistivities are shown in Fig. 7. At $T = 4.2$ K, the thermal energy $k_B T$ is much smaller than the width of the Landau bands. A reference energy spectrum is displayed in Fig. 8. In the explored interval of B_0 values, the cyclotron diameter of the states at the Fermi level

varies between $a/2$ and $a/3$, such that the vertex corrections are very strong.

The contribution of the band conductivity is seen as a central maximum in each of the first three SdH peaks of ρ_{xx} , located in $2.5 \text{ T} < B_0 < 3.15 \text{ T}$. With increasing B_0 these central structures disappear, apparently because the effective disorder broadening Γ_0 increases. Indeed, by increasing the parameter γ the mentioned central maxima decrease, and at the same time the lateral shoulders of ρ_{xx} , as well as ρ_{yy} , increase.

This behavior clearly shows that the scattering conductivity is dominant here. The anisotropy of the scattering conductivities, i. e. $\sigma_{xx} \ll \sigma_{yy}$, or $\rho_{xx} \gg \rho_{yy}$, is an effect *qualitatively* determined by the vertex corrections, and not by the band conductivity. We have already mentioned such an effect in the discussion of Figs. 3 and 4, where it was less pronounced and combined with the presence of a higher band conductivity, but visible even for delta impurities. This type of anisotropy, of the scattering conductivities, cannot be obtained in the CNA. In that approximation again $\sigma_{xx} \approx \sigma_{yy}$ (or $\rho_{xx} \approx \rho_{yy}$), and unlike in the example of the electric modulation, the CNA resistivities become here several times bigger than those plotted in Fig. 7. Our results for the magnetic modulation thus show characteristic similarities with the experimental results of Heisenberg et. al. We are not able to offer a simple argument that could explain the strong anisotropy of the scattering conductivities obtained from the numerical calculations quantitatively. However, we attribute this anisotropy to both the anisotropic electronic states and the anisotropic impurity scattering. Of course, strong anisotropies can be understood qualitatively in the physical picture of quasi-classical orbits with a relaxation of the rigid energy-versus- X_0 dispersion due to disorder broadening (see the discussion in section IV.A of the enhancement of the band conductivity in the middle of a Landau band). Scattering processes that lead to an effective motion in y direction, and thus contribute to σ_{yy}^{scat} , are possible with arbitrarily small changes of the center coordinate X_0 , and are favored if forward scattering predominates. On the other hand, elastic scattering processes leading to a substantial effective motion in x direction require a finite (large) change of the X_0 coordinate, i. e. a scattering by a large angle. Such processes, and consequently their contributions to σ_{xx}^{scat} , are suppressed by predominant forward scattering, and for $2R_c < a$ they become even more improbable, since they require a tunneling through an energy barrier. These aspects have to be better clarified by future analytical calculations.

An analogous set of experimental results has been obtained for an electric modulation of a very short period (32 nm).¹⁴ The resistivity tensor is anisotropic, the resistance in the modulated direction being up to five times bigger than in the uniform direction. The amplitudes of the Shubnikov - de Haas peaks are well represented by Dingle plots, which are specific to unmodulated (homogeneous) systems, where only the scattering conductivity exists. The results suggest that the band conductivity plays no role in these data, and thus the resistance anisotropy is determined by the scattering anisotropy, as we find in our present calculations.

V. CONCLUSIONS AND FINAL REMARKS

We have shown with numerical calculations that for strong magnetic fields the anisotropic character of the electron-impurity scattering has both quantitative and qualitative effects on the resistivity tensor of modulated systems. Our magnetotransport calculation is based on a consistent evaluation of the disorder broadening of the single-particle Green-functions

(and thereby the density of states) and of the Kubo formulas for the conductivity tensor. Formally, the anisotropy effects enter through vertex corrections, which are calculated from the Bethe-Salpeter (integral) equations. In contrast to homogeneous systems, for modulated systems these anisotropy effects are important even for short-range (δ -potential) impurities, if the average magnetic field is so strong that the cyclotron diameter of the electrons at the Fermi level is smaller than the modulation period. Of course, such effects become even much more important for impurities of finite range.

The main results of including the anisotropy effects (vertex corrections) are:

- (1) The band conductivity increases, just like the conductivity of a homogeneous 2DEG for zero magnetic field (which is inversely proportional to the disorder-scattering rate).
- (2) The scattering conductivities decrease, just like the longitudinal conductivities of a homogeneous 2DEG in a high magnetic field (which are proportional to the disorder-scattering rate).
- (3) The scattering conductivity in the direction of the modulation becomes lower than that in the direction perpendicular to the modulation.

The comparison with the available experimental results suggests that the scattering anisotropy is important not only in the classical regime (low B_0)^{9,10}, but also in the quantum case (high B_0). This is seen, in both regimes, in the band conductivity, which has a classical origin, but also in the pure quantum scattering conductivity. Experimental results for both ρ_{xx} and ρ_{yy} in a unidirectional modulation, for high magnetic fields, are however rarely available,^{14,23,24} but still, our results agree qualitatively with these experiments.

The numerical calculations of this work require the solution of the non-linear Dyson equation for the Green operator, and of the linear Bethe-Salpeter equation for the vertex operators, each of which depends on two discrete (Landau) quantum numbers and one quasi-continuous (X_0) quantum number, and in addition on the continuous parameters energy E and B_0 . To make this complex problem tractable with our numerical capabilities, we had to make rather restrictive assumptions for the model parameters. In particular, we assumed a relatively large impurity broadening to ensure a rapid convergence of the Fourier expansions. Therefore, the results shown in this paper are based on a few examples, rather than on a complete insight into the structure of the vertex corrections and a systematic analysis of the length scales imposed by the modulation period, cyclotron radius, and impurity range.

A more detailed, systematic investigation of anisotropic-scattering effects in more realistic cases of high-mobility modulated systems exceeds our present possibilities concerning computer memory and CPU time. Although quantitatively our results depend on the parameters of the Gaussian model for impurities, we believe they do not change qualitatively when the impurity range is increased to more realistic values to simulate the situation at high-mobility semiconductor interfaces. Of course, in that case the realistic impurity model is the Coulomb potential of a charged particle situated outside the 2DEG. Nevertheless, for such a model, in order to avoid singularities in the scattering integrals (A3) or (A6), one has to include the screening effects of the 2DEG on the impurity potential, e.g. within a Thomas-Fermi approximation. Note, that the screening of the periodic lateral potential in the case of the electric modulation may considerably reduce the width of the Landau bands, and thus the influence of VHS on the magnetoresistivities, which we do not expect for a magnetic modulation.^{22,26} On the other hand, the dependence of the screening length on the DOS at the Fermi level, and also the alternating of quasi-metallic (compressible) and insu-

lating (incompressible) phases in strong magnetic fields, open the possibility of describing more complicated, but qualitatively new effects in the resistivities.

ACKNOWLEDGMENTS

A.M. has been supported by Universität Regensburg, under Graduiertenkolleg "Komplexität in Festkörpern" (GK176). Useful discussions with David Heisenberg, Dieter Weiss, and Bernard Etienne are also acknowledged.

APPENDIX A: THE SCBA KERNEL

In the numerical calculation we find it most convenient to use the Landau basis,

$$\langle x, y | nX_0 \rangle = \exp(-iX_0y/\ell^2) \phi_n[(x - X_0)/\ell]/(L_y\ell)^{1/2}, \quad (\text{A1})$$

with $n = 0, 1, 2, \dots$ the orbital (oscillator) quantum number and $X_0 = 2\pi\ell^2 \times (\text{integer})/L_y$ the (quasi-continuous) center coordinate. Eqs. (3.3) and (3.6) have the same structure, which in matrix form reads

$$A_{nm}(X_0) = \sum_{n'm'X'_0} \Gamma_{nm,n'm'}^2(X_0, X'_0) B_{n'm'}(X'_0), \quad (\text{A2})$$

A being either Σ or $I[F]$, and B being either G or F . Due to the translational invariance along y , all these operators are diagonal in X_0 and, similar to the energy spectrum E_{n,X_0} , the X_0 -dependence is periodic with the modulation period a . In the Landau basis the matrix elements of the collision operator depend only on the difference of the center-coordinates,

$$\Gamma_{nm,n'm'}^2(X_0 - X'_0) = n_i \int d\mathbf{R} \langle nX_0 | u(\mathbf{r} - \mathbf{R}) | n'X'_0 \rangle \langle m'X'_0 | u(\mathbf{r} - \mathbf{R}) | mX_0 \rangle, \quad (\text{A3})$$

as can be shown, e.g., by using the Fourier transform \tilde{u} of u . Hence, Eq. (A2) becomes a convolution with respect to X'_0 , and it can be simplified by the Fourier-series expansions

$$B_{n'm'}(X'_0) = \sum_{p \geq 0} b_{n'm'}(p) \cos \left[pKX'_0 + (n' - m' + j) \frac{\pi}{2} \right], \quad (\text{A4})$$

where $K = 2\pi/a$ is the modulation wave vector, and where the phase shifts are chosen to satisfy the reflection symmetry imposed by the modulations: we take $j = 0$ for $B = G$, because $G_{nm}^\sigma(-X_0) = (-1)^{(n-m)} G_{nm}^\sigma(X_0)$, and $j = 1$ for $B = F$, because $F_{nm}^{\sigma\sigma'}(-X_0) = (-1)^{(n-m+1)} F_{nm}^{\sigma\sigma'}(X_0)$. These properties follow for our simple cosine-modulations from the corresponding properties of the matrix elements of the Hamiltonian and of the velocity operator, respectively. Then, Eq. (A2) becomes

$$A_{nm}(X_0) = \sum_{n'm'} \sum_{p \geq 0} b_{n'm'}(p) D_{nm,n'm'}(pK\ell) \cos \left[pKX_0 + (n - m + j) \frac{\pi}{2} \right], \quad (\text{A5})$$

where

$$D_{nm,n'm'}(pK\ell) = \frac{n_i}{\pi\ell^2} \int_0^\infty dq q [\tilde{u}(\frac{q\sqrt{2}}{\ell})]^2 E_{nn'}(q^2) E_{mm'}(q^2) J_{n-n'-m+m'}(pK\ell q\sqrt{2}), \quad (\text{A6})$$

with

$$E_{nm}(z) = \left(\frac{m!}{n!}\right)^{1/2} z^{(n-m)/2} e^{-z/2} L_m^{n-m}(z) = (-1)^{m-n} E_{mn}(z), \quad (\text{A7})$$

$L_n^m(x)$ being the Laguerre polynomials, and $J_n(x)$ the Bessel functions. We have the following properties:

$$D_{nm,n'm'} = (-1)^{n+m+n'+m'} D_{mn,m'n'}, \quad (\text{A8})$$

$$D_{nm,n'm'} = D_{n'm',nm}. \quad (\text{A9})$$

In particular, for delta impurities, i.e., for $\tilde{u}(q) \equiv u_0$, Eq. (A6) can be integrated analytically, and one obtains²⁵

$$D_{nm,n'm'}(pK\ell) = \frac{n_i u_0^2}{2\pi\ell^2} E_{nm}(p^2 z) E_{n'm'}(p^2 z), \quad (\text{A10})$$

where $z = (K\ell)^2/2$.

Using the Fourier series (A5) in Eqs. (3.3) and (3.6), we solve iteratively the self-consistent equations (3.2)-(3.3) and (3.5)-(3.6), starting from the CNA. The velocity matrix elements, used in Eqs. (3.5) and (3.4), are

$$\langle n' X_0 | v_\alpha | n X_0 \rangle = \eta_\alpha \frac{\ell\omega_c}{\sqrt{2}} \left(\sqrt{n+1} \delta_{n',n+1} + \eta_\alpha^2 \sqrt{n'+1} \delta_{n,n'+1} \right), \quad (\text{A11})$$

with the notation $(\eta_x, \eta_y) = (i, 1)$.

One can directly show the following symmetries:

$$(F_\alpha^{\sigma\sigma'})_{mn}^* = (F_\alpha^{-\sigma'-\sigma})_{nm}, \quad (\text{A12})$$

for both $\alpha = x, y$, and from the symmetries of the Hamiltonian, which in the Landau representation is a real, symmetric matrix, and of the velocity operators, see Eq. (A11), also

$$(F_x^{\sigma\sigma'})_{mn} = -(F_x^{\sigma'\sigma})_{nm}, \quad (\text{A13})$$

and

$$(F_y^{\sigma\sigma'})_{mn} = (F_y^{\sigma'\sigma})_{nm}. \quad (\text{A14})$$

Analog properties occur also for the matrix elements of the operators $I[F_\alpha^{\sigma\sigma'}]$. In particular, for delta impurities we have in addition

$$(I[F_\alpha^{\sigma\sigma'}])_{mn} = (I[F_\alpha^{\sigma'\sigma}])_{nm}, \quad (\text{A15})$$

which implies $I[F_x^{\sigma\sigma}] = 0$.

APPENDIX B: SOME CNA RESULTS

The matrix elements of the electric modulation potential $V(x) = U \cos(KX_0)$ in the Landau representation are²⁶

$$V_{mn}(X_0) = U E_{mn} \left(\frac{1}{2} \ell^2 K^2 \right) \cos \left(KX_0 + (m - n) \frac{\pi}{2} \right), \quad (\text{B1})$$

with $E_{mn}(z)$ defined in Eq. (A7). For weak modulation, perturbation expansion yields to lowest order in U

$$E_{n,X_0}^{(1)} = \epsilon_n + U E_{nn} (\ell^2 K^2 / 2) \cos(KX_0), \quad (\text{B2})$$

with $\epsilon_n = \hbar\omega_c(n+1/2)$. Since for $R_n \equiv \ell\sqrt{2n+1} \gg 1/K$ one has the asymptotic expression⁴ $E_{nn}(\ell^2 K^2 / 2) \approx \cos(KR_n - \pi/4) / (\pi KR_n / 2)^{1/2}$, one expects flat Landau bands, if the *flat-band condition* $2R_n = a(\lambda - 1/4)$ holds for a $\lambda = 1, 2, \dots$. The states of the modulated basis are,⁴ to first order in U ,

$$|nX_0\rangle^{(1)} = |nX_0\rangle + \sum_{n' \neq n} |n'X_0\rangle \frac{V_{n'n}(X_0)}{\epsilon_n - \epsilon_{n'}}. \quad (\text{B3})$$

In first order of U , this leads to a non-vanishing diagonal matrix element of v_y in the modulated basis, given by $\langle nX_0 | v_y | nX_0 \rangle = -(\hbar\omega_c)^{-1} dE_{n,X_0}^{(1)} / dX_0$. For the off-diagonal velocity matrix elements one obtains

$$|\langle mX_0 | v_\alpha | nX_0 \rangle|^2 = |\langle mX_0 | v_\alpha | nX_0 \rangle|^2 + O(U / \hbar\omega_c), \quad (\text{B4})$$

where the leading contributions $|\langle mX_0 | v_\alpha | nX_0 \rangle|^2$ are independent of U and identical for v_x and v_y , see Eq. (A11). Thus, for weak modulation the scattering conductivities σ_{xx}^{scat} and σ_{yy}^{scat} are approximately the same. For stronger modulation this is no longer true, even within the CNA.

Within the CNA the imaginary part of Eq. (3.3) reads

$$\text{Im} \Sigma^-(E) = \Gamma_0^2 \sum_n \int_0^a \frac{dX_0}{a} \text{Im} G_{nn}^-(X_0, E), \quad (\text{B5})$$

and the DOS is given by $D(E) = D_0 \text{Im} \Sigma^-(E) / (\pi \Gamma_0^0)$. For an estimate of the scattering and band conductivities we assume that the collision broadening $\text{Im} \Sigma^-(E)$ of the spectral functions $\text{Im} G_{nn}^-(X_0, E) / \pi$ is much smaller than the modulation-induced bandwidth ($\sim U |E_{nn}(\ell^2 K^2 / 2)|$), and that the latter is much smaller than $\hbar\omega_c$. Then the dominant contribution to Eq. (3.8) comes from the Landau bands at the energy E . Let us assume that E lies in the band n_F , so that $|E - E_{n_F, X_0} - \text{Re} \Sigma(E)| \ll \hbar\omega_c$. Then, the leading order contributions to the scattering conductivity are obtained for $n = n_F$ and $n' = n_F \pm 1$ (and n and n' interchanged), and we may approximate

$$\text{Im} G_{n'n'}^-(X_0, E) \approx \text{Im} \Sigma^-(E) / (\hbar\omega_c)^2, \quad (\text{B6})$$

Inserting this and the off-diagonal velocity matrix elements from Eq. (A11), we obtain

$$\sigma_{\alpha\alpha}^{scat}(E) \approx \frac{e^2}{h} (2n_F + 1) \frac{\Gamma_0^0}{\hbar\omega_c} \left[\frac{D(E)}{D_0} \right]^2. \quad (\text{B7})$$

This is a general result and holds for unmodulated systems¹⁶ and for a 2DEG with a two-dimensional superlattice as well.²⁷ It shows that the scattering conductivity is proportional to the *scattering rate* $1/\tau_{sc} = \Gamma_0^0/2\hbar$, and that its maxima and minima follow those of the DOS.

The band conductivity σ_{yy}^{band} is dominated by the term containing the square of the spectral function $\text{Im} G_{n_F n_F}^-(X_0, E)/\pi$. Considered as a function of X_0 , the latter has δ -function-like peaks at the values X_F satisfying

$$E - E_{n_F, X_F} - \text{Re}\Sigma(E) = 0. \quad (\text{B8})$$

To obtain an estimate (actually an upper limit) of σ_{yy}^{band} , we take the square of the velocity matrix elements and one of the $\text{Im} G_{n_F n_F}^-(X_0, E)$ factors at $X_0 = X_F$, i.e., we approximate $\text{Im} G_{nn}^-(X_0, E) \approx \text{Im} G_{n_F n_F}^-(X_F, E) = 1/\text{Im}\Sigma^-(E)$. Then we obtain with Eqs. (3.8) and (3.9)

$$\sigma_{yy}^{band}(E) \approx \frac{e^2}{h} \left| \frac{2\ell}{\Gamma_0} \frac{dE_{n_F, X_0}}{dX_0} \right|_{X_0=X_F}^2, \quad (\text{B9})$$

which according to Eq. (B8) depends on E (at $T \rightarrow 0$ on E_F), via $X_F = X_F(E)$. This shows already, that $\sigma_{yy}^{band}(E)$ is proportional to the *scattering time* $2\hbar/\Gamma_0^0$, and that it becomes small for flat bands and near the band edges, where the energy dispersion becomes flat. This is opposite to the DOS, which becomes large at flat bands and near the band edges (VHS).

If Eq. (B8) holds for E well within a Landau band, i.e., sufficiently far from the band edges, we may approximate $\text{Im} G_{n_F n_F}^-(X_0, E)/\pi \approx \delta(X_0 - X_F)/|dE_{n, X_0}/dX_0|_{X_0=X_F}$ to obtain

$$D(E) \approx 2/[\pi a \ell^2 |dE_{n_F, X_0}/dX_0|_{X_0=X_F}], \quad (\text{B10})$$

where we assumed that Eq. (B8) is satisfied at $X_0 = \pm X_F$. Inserting this into Eq. (B9) yields

$$\sigma_{yy}^{band}(E) \sim \frac{e^2}{h} \frac{\hbar\omega_c}{\Gamma_0^0} \left[\frac{4\ell D_0}{aD(E)} \right]^2, \quad (\text{B11})$$

which is a reasonable estimate at energies well inside the modulation-induced Landau bands.

If we repeat the analysis of the band conductivity for overlapping Landau bands, i. e. if we drop the condition for the bandwidth $U |E_{nn}(\ell^2 K^2/2)| \ll \hbar\omega_c$ we arrive at

$$\sigma_{yy}^{band}(E) \approx \frac{e^2}{h} \left(\frac{2\ell}{\Gamma_0} \right)^2 \frac{\left| \sum_n \frac{dE_{n, X_0}}{dX_0} \right|_{E_{n, X_0}=E}}{\left| \sum_{n'} \left(\frac{dE_{n', X_0}}{dX_0} \right)^{-1} \right|_{E_{n', X_0}=E}}, \quad (\text{B12})$$

The difference of this expression to Eq. (B9) is the contribution of more than one Landau band at the same time to the total density of states (denominator) and of bands with differing group velocities to the conductivity (numerator).

REFERENCES

- ¹ D. Weiss, K. v. Klitzing, K. Ploog, and G. Weimann, *Europhys. Lett.* **8**, 179 (1989).
- ² P. H. Beton, E. S. Alves, P. C. Main, L. Eaves, M. W. Dellow, M. Henini, O. H. Hughes, S. P. Beaumont, and C. D. W. Wilkinson, *Phys. Rev. B* **42**, 9229 (1990).
- ³ R. R. Gerhardts, D. Weiss, and K. v. Klitzing, *Phys. Rev. Lett.* **62**, 1173 (1989); R. W. Winkler, J. P. Kotthaus, and K. Ploog, *ibid* **62**, 1177 (1989); P. Vasilopoulos and F. M. Peeters, *ibid* **63**, 2120 (1989).
- ⁴ C. Zhang and R. R. Gerhardts, *Phys. Rev. B* **41**, 12850 (1990).
- ⁵ D. P. Xue and G. Xiao, *Phys. Rev. B* **45**, 5986 (1992); F. M. Peeters and P. Vasilopoulos, *ibid* **46**, 4667 (1992).
- ⁶ Q. W. Shi and K. Y. Szeto, *Phys. Rev. B* **43**, 12990 (1996).
- ⁷ C. W. J. Beenakker, *Phys. Rev. Lett.* **62**, 2020 (1989).
- ⁸ R. R. Gerhardts, *Phys. Rev. B* **53**, 11064 (1996).
- ⁹ R. Menne and R. R. Gerhardts, *Phys. Rev. B* **57**, 1707 (1998).
- ¹⁰ A. D. Mirlin and P. Wölfle, *Phys. Rev. B* **58**, 12986 (1998).
- ¹¹ D. Weiss, K. v. Klitzing, K. Ploog, and G. Weimann, *Surf. Sci.* **229**, 88 (1990).
- ¹² M. Tornow, D. Weiss, A. Manolescu, R. Menne, K. v. Klitzing, and G. Weimann, *Phys. Rev. B*, **54**, 16397 (1996).
- ¹³ P. D. Ye, D. Weiss, R. R. Gerhardts, K. v. Klitzing, and S. Tarucha, *Physica B* **249-251**, 330 (1998).
- ¹⁴ F. Petit, M. Hayne, F. Lelarge, and B. Etienne, *Physica B* **249-251**, 922 (1998).
- ¹⁵ O. Steffens, T. Schlösser, P. Rotter, K. Ensslin, M. Suhrke, J. P. Kotthaus, U. Rössler, and M. Holland, *J. Phys. Cond. Matt.* **10**, 3859 (1998).
- ¹⁶ T. Ando, A. B. Fowler, and F. Stern, *Rev. Mod. Phys.* **54** 437 (1982).
- ¹⁷ S. D. M. Zwerschke, A. Manolescu, and R. R. Gerhardts, *Phys. Rev. B* **60**, 5536 (1999)
- ¹⁸ R. R. Gerhardts and J. Hajdu, *Z. Phys. B* **245**, 126 (1971).
- ¹⁹ R. R. Gerhardts, *Z. Phys. B* **22**, 327 (1975).
- ²⁰ Y. Tan, *Phys. Rev. B*, **49**, 1827 (1994).
- ²¹ G. R. Aizin and V. A. Volkov, *Zh. Eksp. Teor. Fiz.* **87**, 1469 (1984) [*Sov. Phys.-JETP* **60**, 844 (1984)]
- ²² A. Manolescu and R. R. Gerhardts, *Phys. Rev. B*, **56**, 9707 (1997).
- ²³ D. Heisenberg, Ph.D. Thesis, Universität Stuttgart and Max-Planck-Institut für Festkörperforschung Stuttgart (1998).
- ²⁴ D. Heisenberg, D. Weiss, K. v. Klitzing, M. Behet, J. D. Boeck, and G. Borghs, to be published.
- ²⁵ I. S. Gradshteyn and I. M. Ryzhik, *Table of Integrals, Series, and Products*, Academic Press (1994).
- ²⁶ U. J. Gossmann, A. Manolescu, and R. R. Gerhardts, *Phys. Rev. B*, **57**, 1680 (1998).
- ²⁷ R. R. Gerhardts, D. Weiss, and U. Wulf, *Phys. Rev. B*, **43**, 5192 (1991)

FIGURES

FIG. 1. Diagrams for the generalized SCBA: Dyson [(3.2) and (3.3)] and Bethe-Salpeter [(3.5) and (3.6)] equations.

FIG. 2. (a) Density of states at the Fermi level for the electric modulation, $D_0 = m/(\pi\hbar^2)$. (b) The energy spectrum for $B_0 = 0.81$ T. The dashed horizontal line shows the Fermi level.

FIG. 3. Conductivities for the electric modulation.

FIG. 4. Resistivities for the electric modulation.

FIG. 5. Resistivities for the magnetic modulation in the regime of high band conductivity.

FIG. 6. (a) Energy spectra for the magnetic modulation with GaAs parameters, corresponding to Fig. 5. (b) The density of states at the Fermi level for $r_0 = 10$ nm.

FIG. 7. Resistivities for the magnetic modulation in the regime of low band conductivity.

FIG. 8. An energy spectrum for the magnetic modulation with InAs parameters, corresponding to Fig. 7, with $B_0 = 3$ T.

Fig. 1

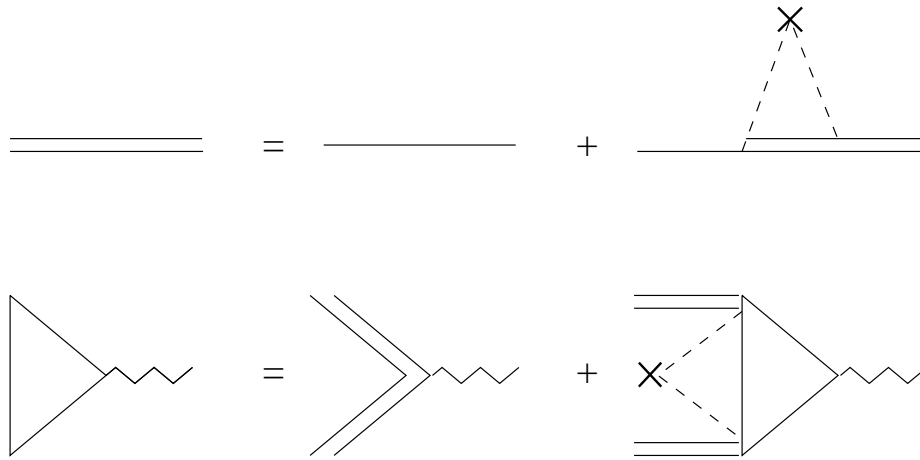


Fig.2

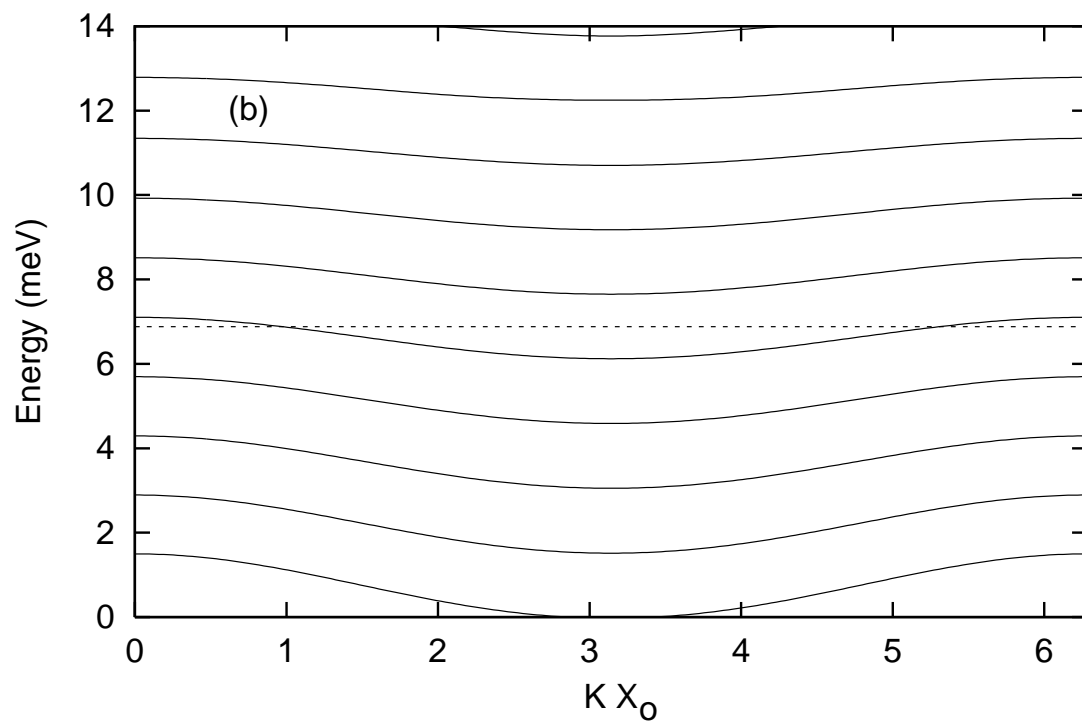
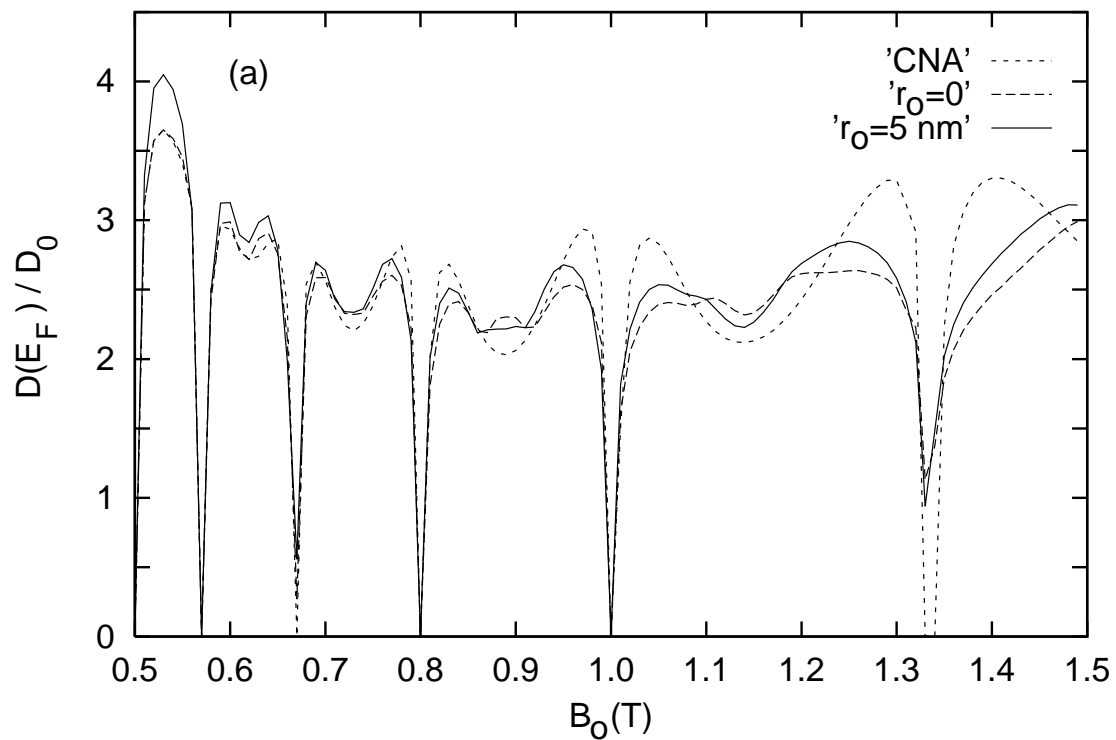


Fig.3

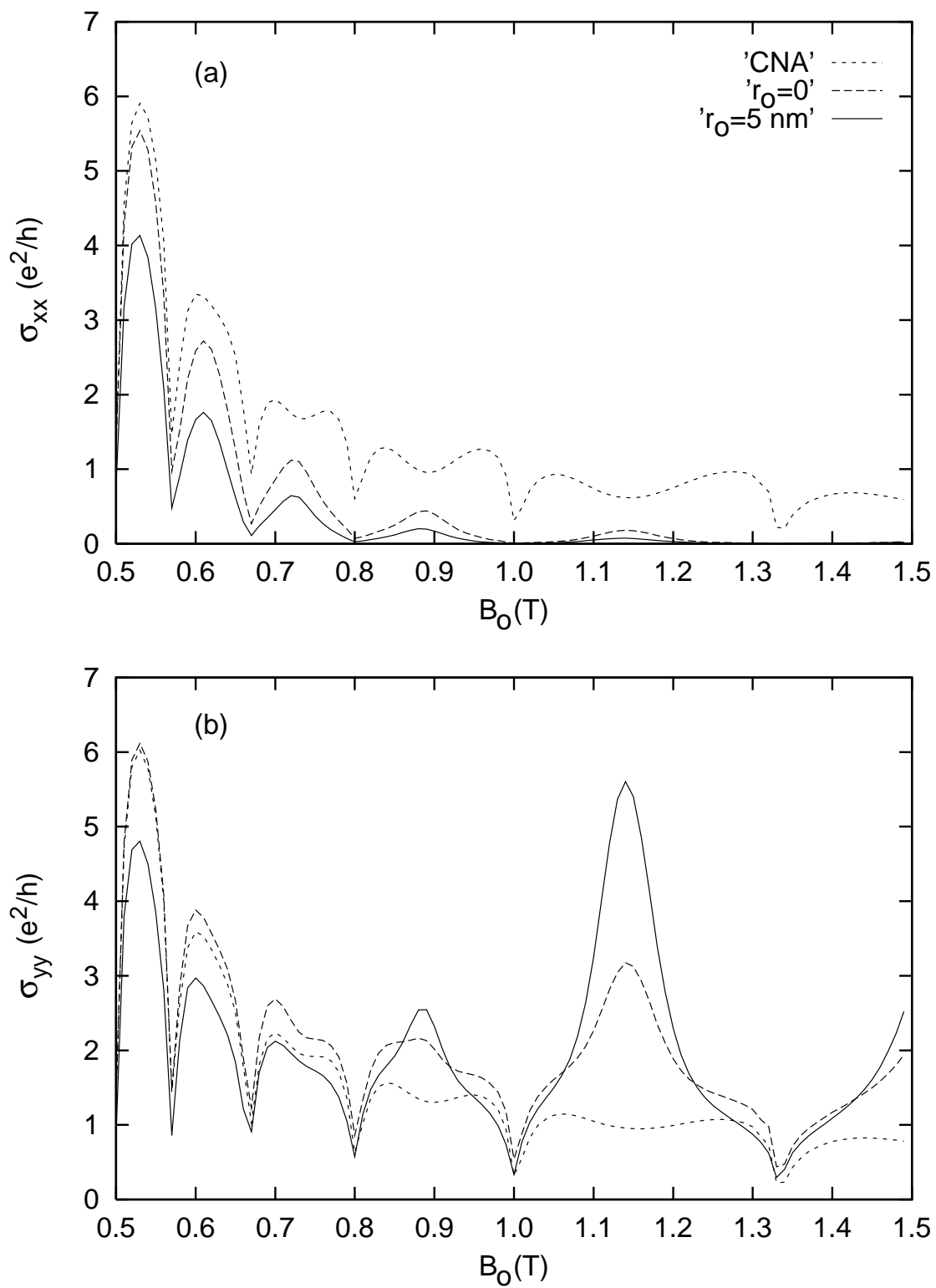


Fig.4

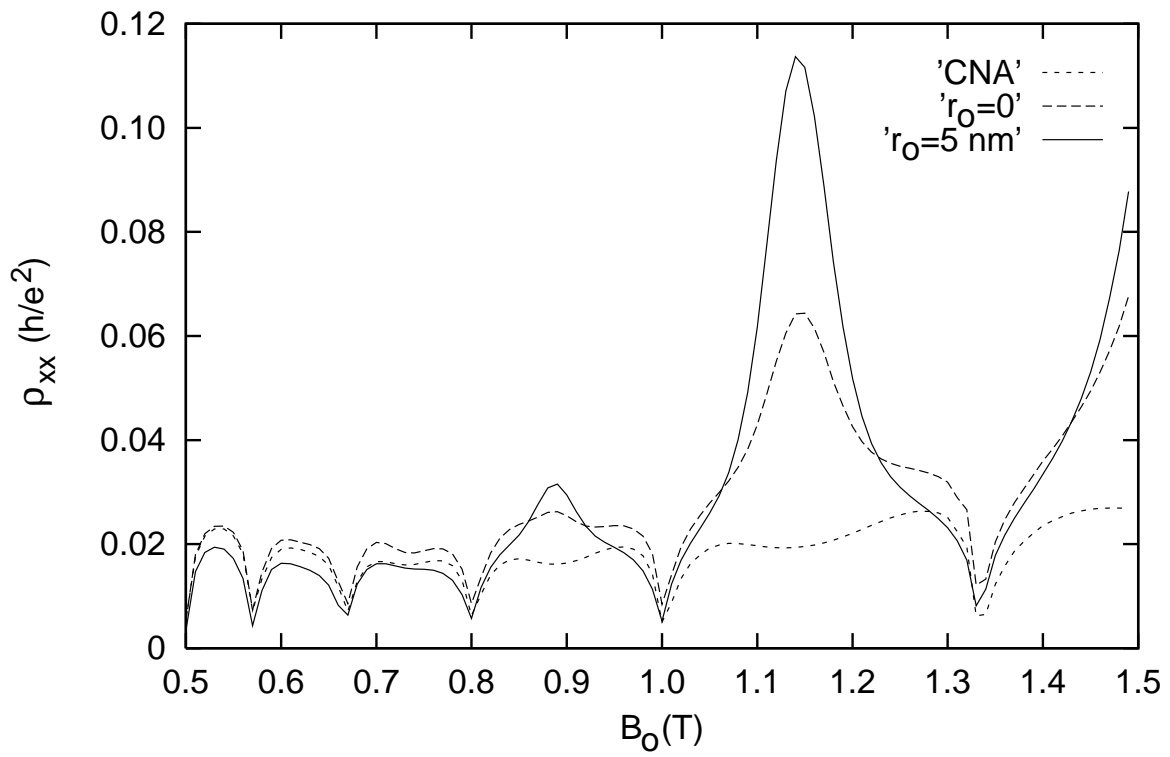


Fig.5

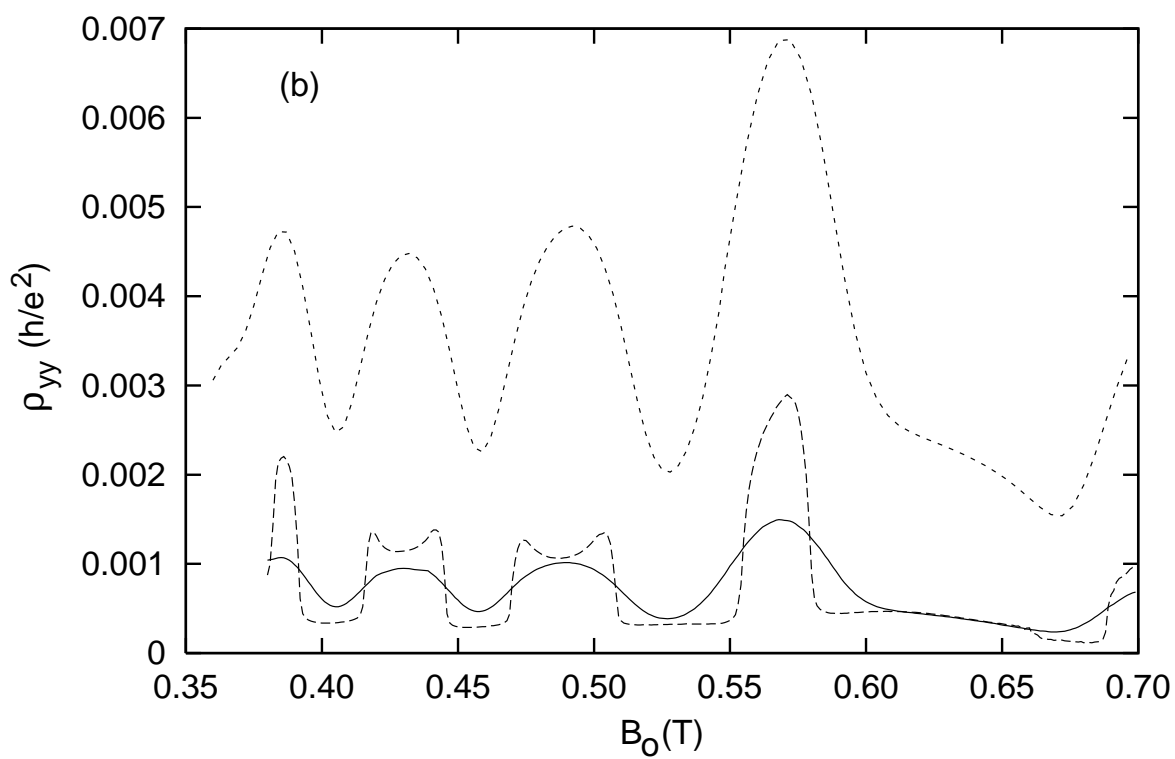
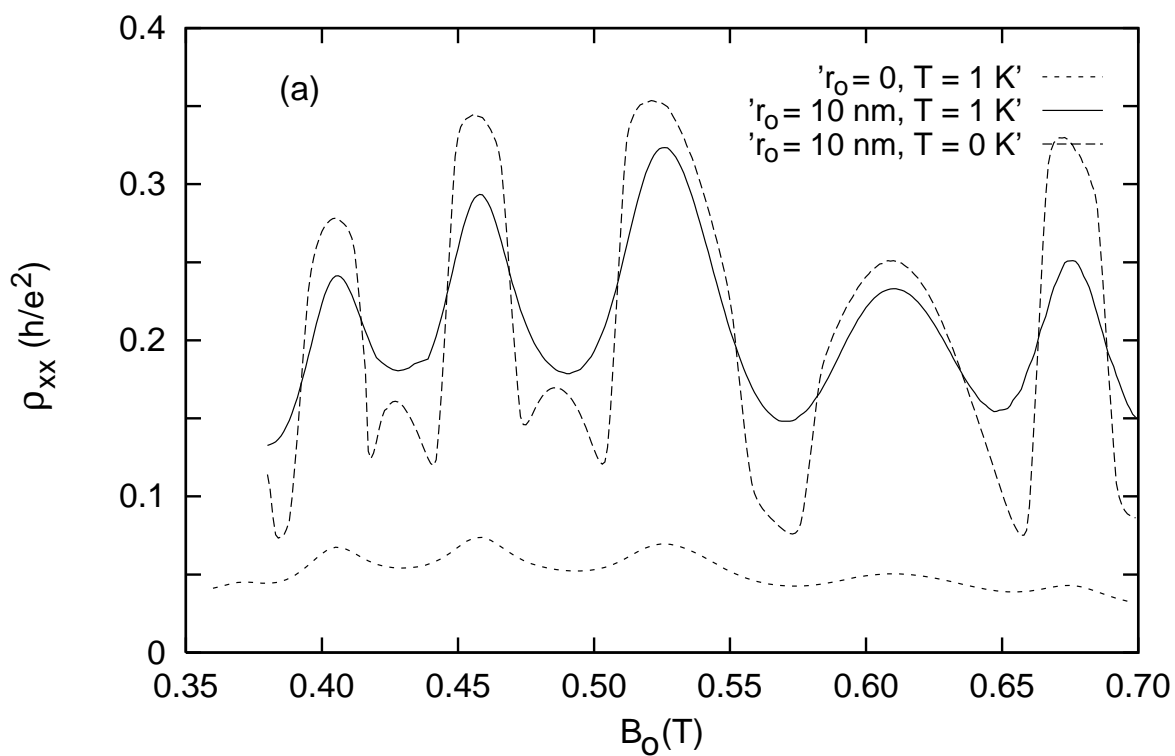


Fig.6 (a)

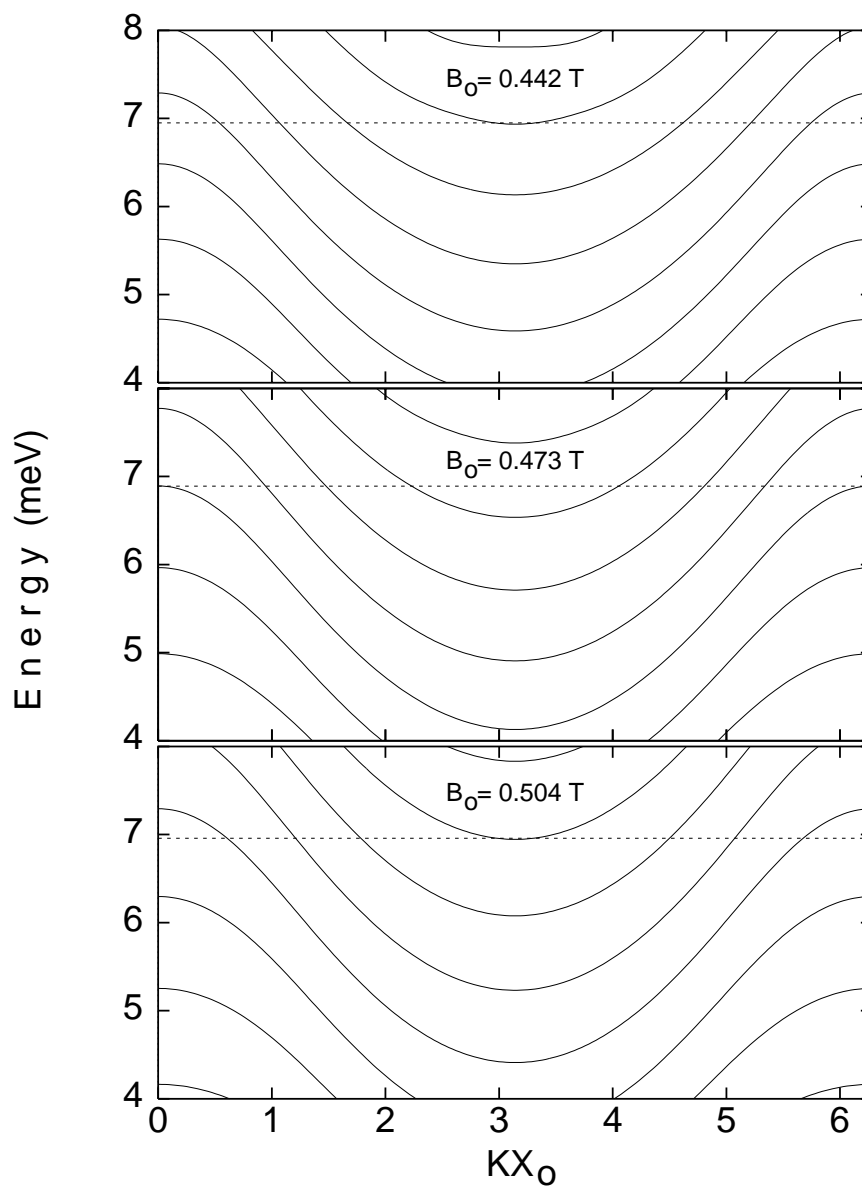


Fig.6 (b)

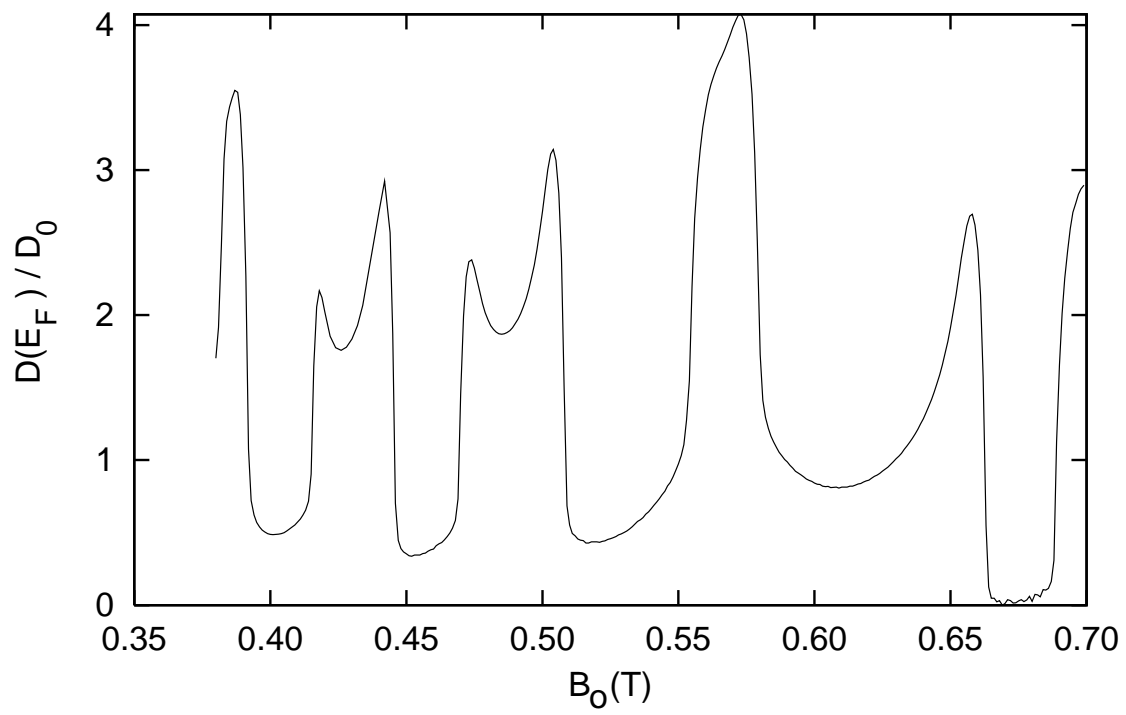


Fig.7

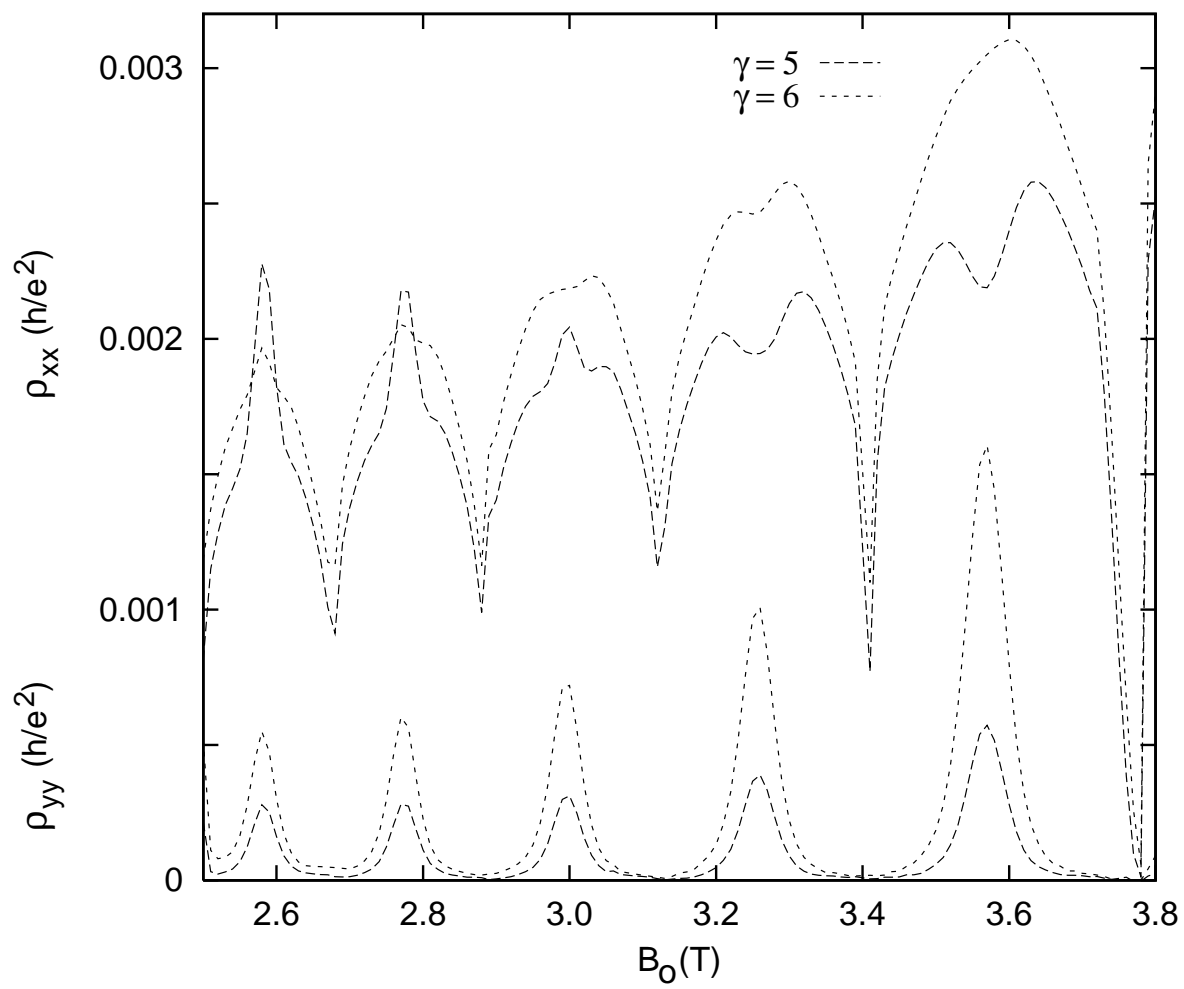


Fig.8

